Journal of Nuclear Medicine, published on March 16, 2017 as doi:10.2967/jnumed.116.188896

^{18}F-GP1, a novel fluorine-18 labeled tracer designed for PET imaging of thrombi with high detection sensitivity and low background

Jessica Lohrke[1], Holger Siebeneicher[1], Markus Berger[1], Michael Reinhardt[1], Mathias Berndt[2], Andre Mueller[2], Marion Zerna[2], Norman Koglin[2], Felix Oden[2], Marcus Bauser[1], Matthias Friebe[2], Ludger M. Dinkelborg[2], Joachim Huetter[1], Andrew W. Stephens[2]

1) Bayer AG, Drug Discovery, Muellerstrasse 178, 13353 Berlin, Germany

2) Piramal Imaging GmbH, Tegeler Str. 6-7, 13353 Berlin, Germany

Word count: 5063/5000

Running title: Small molecule PET imaging of thrombus

Funding: The trial was funded by Bayer Pharma AG and Piramal Imaging GmbH, Berlin, Germany.

First author:
Jessica Lohrke, PhD, Bayer AG
Muellerstrasse 178, 13353 Berlin, Germany
jessica.lohrke@bayer.com
Phone: +49-3046814772

Corresponding author:
Andrew W. Stephens, MD, PhD, Piramal Imaging GmbH
Tegeler Straße 6-7, 13353 Berlin, Germany
andrew.stephens@piramal.com
Phone: +49-30461124603
Fax: +49-30461124629

ABSTRACT

Thromboembolic diseases such as myocardial infarction, stroke, transient ischemic attacks and pulmonary embolism are major causes of morbidity and mortality worldwide. GPIIb/IIIa is the key receptor involved in platelet aggregation and is a validated target for therapeutic approaches and diagnostic imaging. The aim of this study was to develop and characterize a specific small molecule tracer for positron emission tomography (PET) imaging that binds with high affinity to GPIIb/IIIa receptors and has suitable pharmacokinetic properties to overcome limitations of previous approaches.

Methods. Binding of ^{18}F-GP1 to GPIIb/IIIa receptors was investigated in competition binding assays and autoradiography using a fresh cardiac thrombus from an explanted human heart. The clot-to-blood-ratio for ^{18}F-GP1 was investigated by an *in vitro* blood flow model. Biodistribution and thrombus detection was investigated in cynomolgus monkeys after insertion of a roughened catheter into either the vena cava or aorta.

Results. ^{18}F-GP1 is a novel fluorine-18 labeled small molecule for PET imaging of thrombi. The IC_{50} of ^{18}F-GP1 to GPIIb/IIIa was determined to be 20nM. ^{18}F-GP1 binds to thrombi with a mean clot-to-blood ratio of 95. Binding is specific and can be displaced by excess non-radioactive derivative. Binding is not effected by anticoagulants such as aspirin or heparin. ^{18}F-GP1 shows rapid blood clearance and a low background after i.v. injection in cynomolgus monkeys. Small arterial, venous thrombi, thrombotic depositions on damaged endothelial surface and small cerebral emboli were detected *in vivo* by PET imaging.

Conclusions. ^{18}F-GP1 binds specifically with high affinity to the GPIIb/IIIa receptor involved in platelet aggregation. Due to its favorable pre-clinical characteristics, ^{18}F-GP1 is currently being investigated in a human clinical study.

Key Words: imaging, platelets, embolism, thrombosis, glycoproteins

INTRODUCTION

Venous and arterial thrombi play an important role in various vascular pathologies such as myocardial infarction, stroke, transient ischemic attacks, deep vein thrombosis (DVT), and pulmonary embolism (PE) (*1*). These thromboembolic diseases are a major cause of morbidity and mortality worldwide. Currently available diagnostic techniques of thrombus imaging rely on different modalities depending on the vascular territory. For example, ultrasound is used for detection of DVT (*2*) and carotid stenosis (*3*), trans-esophageal echocardiography and contrast-enhanced magnetic resonance imaging for cardiac chamber clots (*4*), and contrast media enhanced computed tomography pulmonary angiography has become the gold standard for the detection of PE (*5,6*).

Limitations remain in the tests to diagnose venous clots in DVT and PE; an agent would be very valuable that could visualize both (*7*). In addition, standard imaging modalities generally do not allow for reliable discrimination between fresh unstable thrombi and chronic organized thrombi. Imaging of DVT with ultrasound is limited to proximal large vein disease and is unable to distinguish active thrombotic processes in the context of recurrent disease, nor does it have high sensitivity in distal or small vessel disease (*8*). Computed tomography pulmonary angiography has demonstrated acceptable sensitivity for PE, although the sensitivity decreases in the acute setting and as the location of the PE becomes more distal (*9*). Underdiagnosis of PE remains a problem as evidenced by the fact that approx. 30% of hospital deaths are complicated by unsuspected PE (*10*).

As a result of arterial thrombi, every year worldwide about 33 million patients experience a new or a recurrent stroke. A highly sensitive molecular imaging approach could potentially identify activated platelets in the presence of atherosclerotic plaques, a harbinger of thromboembolic events. Current imaging modalities rely on structural characteristics, such as vascular flow impairment, and do not address the critical molecular components of the thrombus.

To overcome these diagnostic limitations new molecular targets and imaging approaches need to be explored. The glycoprotein IIb/IIIa (GPIIb/IIIa) receptor has historically represented an interesting target for drug development as it is a key player in the thrombus formation. Activated platelets express a high number of this receptor (40,000-80,000 per platelet) (*11*). GPIIb/IIIa is a member of the integrin family of cell surface proteins and also known as $\alpha_{IIb}\beta_3$. It undergoes allosteric activation on stimulation of the platelet by a variety of agents (e.g. thrombin, adenosine diphosphate, thromboxane). In a growing thrombus, the key step of platelet aggregation is characterized by the binding of activated GPIIb/IIIa to blood fibrinogen domains containing the arginine-glycine-aspartic acid (RGD) motif, which results in crosslinking. The design and development of glycoprotein IIb/IIIa inhibitors has attracted a considerable amount of interest in pharmacological research with respect to anti-platelet and anti-thrombotic activity (*12-17*). GPIIb/IIIa antagonists are commercially available, e.g. abciximab (ReoPro, Centocor, Eli Lilly), eptifibatide (Integrilin, GlaxoSmithKline) and tirofiban (Aggrastat, Correvio International Sarl). Tirofiban and eptifibatide are both synthetic RGD peptidomimetics.

Several radiotracer-based diagnostic approaches have been explored previously including targeting of GPIIb/IIIa (*18*). For example, ^{99m}Technetium labeled peptide apcitide (^{99m}Tc-Acutect®) (*19*) contains an RGD binding motif and was developed as a single photon emission computed tomography tracer for the detection of DVT. It received FDA approval for this indication but was later abandoned. ^{99m}Tc-Fab against D-Dimer progressed to Phase2 (*20,21*) and preclinical studies with ^{64}Cu-labeled peptides binding to fibrin have recently been described (*22*). Main limitations of agents previously investigated in the clinic were low target-to-background ratios, slow clearance and inability to distinguish acute versus chronic disease (*18*).

The aim of this study was to develop and characterize a novel small molecule for thrombus PET-imaging that has a high affinity to GPIIb/IIIa receptors as well as low background and rapid blood clearance . The preclinical results from a novel ^{18}F-labelled ‘fiban’-class ligand called ^{18}F-GP1 are presented here.

MATERIALS AND METHODS

Synthesis of ^{18}F-GP1

^{18}F-GP1 was synthesized by nucleophilic radiofluorination starting from the protected tosylate precursor. The radiolabel was introduced directly before deprotection of the precursor molecule and subsequent purification (Fig. 1).

In vitro characterization of ^{19}F-GP1 and ^{18}F-GP1

GPIIb/IIIa binding assay. The IC_{50} value of the non-radioactive ^{19}F-GP1 was determined by an *in vitro* competition assay using microtiter plates coated 48hr with 5µg/mL purified human GPIIb/IIIa (Enzyme Research Laboratories) in PBS. The nonspecific antibody binding sites were blocked (Roti-Block, Roth). The plates were incubated with 30nM ^{3}H-elarofiban (289GBq/mmol, Bayer Isotope Chemistry) and a dilution series of ^{19}F-GP1 ranging from 0.1 to 2000nM in quadruplicate. After 60min incubation the plates were washed three times with 200µL PBS/well. The wells were filled with 140µL scintillation cocktail (Microscint40, Perkin-Elmer). After shaking for 15min, plates were measured using a TopCount-NXTv2.13 (Perkin-Elmer). The resulting IC_{50}-value represents the mean of three independent assays. The platelet aggregation assay was performed as described previously (*23*). Human platelet-rich plasma was investigation after stimulus of adenosine diphosphate and platelet clumping recorded as a dynamic measure.

Autoradiography of an explanted human thrombus. Binding of ^{18}F-GP1 to a human thrombus was investigated by autoradiography on a cardiac thrombus from an explanted human heart (gift from the

Herz- und Diabeteszentrum, Bad Oeynhausen, Germany). The fresh thrombus from the right ventricle was embedded in Tissue-Tek and 18µm cryosections were incubated with ^{18}F-GP1 (50Bq/µL in HEPES, 0.1% BSA, 100µl per slice) for 1hr at room temperature, rinsed 3-times with HEPES and left over night for exposure on BAS-SR Imaging plates (Fuji). A competition experiment was performed by adding an excess of tirofiban (0.5µg/mL, Sigma) to the ^{18}F-GP1 solution. CD41 (GPIIb) staining was performed with the anti-CD41 antibody from abcam (ab11024) with the AP-fast red detection system.

In vitro blood flow model. The binding of ^{18}F-GP1 to thrombi was investigated in an *in vitro* blood flow model, modified from the method described by Sukavaneshvar (*24*). An open tube-set consisting of tygon-tubes (R-1000, inner diameter 3.2mm), an open reservoir and a chamber made of a piece of polyethylene-tube (PE160, Intramedic) was used. The chamber contained a loop with a roughened nylon fishing line for thrombus formation (thrombogenic surface prepared with sandpaper). A peristaltic-pump was used for blood circulation. The flow in the middle of the thrombus chamber was adjusted to 70-90cm per second, monitored by an ultrasound-Doppler measurement. 10mL fresh blood was taken from a volunteer using citrate-tubes (Sarstedt S-Monovette) and immediately laid into an incubator at a temperature of 37°C (Heraeus miniTherm). The thrombus formation was initiated by the addition of 0.75mL 2%$CaCl_2$-solution in the 15ml tube-set (final concentration 10mM $CaCl_2$). After 7min of thrombus formation, ^{18}F-GP1 (0.5-1.0MBq) was added. The re-calcified blood and ligand were circulated for another 3min (tracer incubation time). After 10min the pump was stopped, aliquots were taken and measured in a gamma counter (Wizard3, Perkin-Elmer). The thrombus was removed together with the roughened thread from the thrombus-chamber and both were rinsed with saline, measured in a gamma counter, dried and weighted. In some studies the calcified blood was exchanged with buffer or fresh blood after 3min of tracer incubation to simulate tracer washout conditions.

The impact of anticoagulants on ^{18}F-GP1 thrombus binding was investigated with blood from a donor, who had taken 600mg acetylsalicylic acid (aspirin) 24hr prior to investigation by the *in vitro* thrombus model described above. In another experiment, the blood of a donor was collected in tubes prepared with heparin (2I.E./mL blood). ^{99m}Technetium labeled apcitide (^{99m}Tc-Acutect®) (*19*) was also investigated in this model for comparison. From each individual blood donor multiple independent studies were performed. Studies in which clots had a weight of >0.1mg were used for the calculation of clot-blood ratios.

In vitro PET study. The *in vitro* blood thrombus model described above was combined with a PET camera (Siemens Inveon PET/CT) to investigate the capability to image of ^{18}F-GP1 thrombus binding. The part of the tube set that contained the thrombus was placed inside the PET camera. The thrombus was imaged continuously from the addition of the tracer up to 60min post injection. To simulate tracer washout conditions, 3min after tracer incubation the blood was exchanged with new citrated blood after 10min. In one set of experiments excess non-radioactive ^{19}F-GP1 (2.8µM) was added after 30min to study displacement.

PET imaging studies in cynomolgus monkeys

The animals were handled in compliance with German animal welfare legislation, and the experiments were performed with the approval of the state animal welfare committee. *In vivo* binding studies were performed in cynomolgus monkeys (*Macaca fascicularis*, female, R.C. Hartelust BV, n=3). Prior to interventions, the animals were anesthetized with an i.m. injection of a mixture of Xylazin (0.12 mL/Kg, Rompun®, Bayer HealthCare) and Ketamine (0.12mL/Kg Ketavet®, Pfizer). Buprenorphine (6µg/kg) was administered i.m. as analgesia.

A roughened polyethylene tube was advanced into either the thoracic aorta via the carotid artery and/or the vena cava via the femoral vein 30min prior tracer administration. The animals were placed inside the PET-camera (Siemens Inveon PET/CT) and 25MBq/animal of ^{18}F-GP1 were administered intravenously. Dynamic PET images of the thorax were acquired from 0-60min post injection. Subsequently static images were acquired for 10min of the brain and the lower abdomen. After finishing the PET data acquisition, the catheter was removed and the thrombus was weighed and counted in the gamma counter. The animals were sacrificed by phenobarbital treatment prior to recovery from anesthesia. For organ distribution, parts of all important organs (liver, kidney, lung, spleen) and body fluids (blood, gall, urine) were removed, weighed and the activity determined with a gamma counter. PET data were reconstructed using the OSEM-2D algorithm and analyzed with the software package provided by the scanner manufacturer. A 3D volume-of-interest was manually drawn for quantification of uptake and kinetic analyses.

RESULTS

In vitro characterization of ^{19}F-GP1 and ^{18}F-GP1

^{19}F-GP1 binds to purified human GPIIb/IIIa receptor with an IC_{50} value of 20nM in a competition assay against ^{3}H-elarofiban (Fig. 2A). An IC_{50} of 19nM was measured for elarofiban in the same assay. The inhibition of platelet aggregation was investigated by using human platelet-rich plasma. In this assay, an IC_{50} of 43nM was determined for tirofiban and 147nM for ^{19}F-GP1 (Supplemental Fig. 1). The ability of ^{18}F-GP1 to bind to an explanted human thrombus from the left ventricle was analyzed by autoradiography. After incubation with ^{18}F-GP1 a strong signal bound to the thrombus was observed that can be fully displaced by competition with excess GPIIb/IIIa ligand. CD41 (GPIIb) staining of the slices confirmed that ^{18}F-GP1 binds in regions with cellular platelet deposition (Fig. 2B).

As binding to isolated receptors and on tissue slides is static, the binding characteristics of ^{18}F-GP1 were investigated during circulation in a less artificial environment. An *in vitro* blood flow model was established, which allows thrombus formation under standardized conditions (Figs. 3A and 3B). In this model, ^{18}F-GP1 showed a strong accumulation at the site of thrombus formation. The binding was specific and could be blocked by addition of an excess of elarofiban. Clots in this model were CD41 positive by IHC (data not shown). The average clot-to-blood ratio was 95.2±50.2 for ^{18}F-GP1 and 35.2±17.6 for apcitide (Fig. 3C). The impact of therapeutics to prevent blood clots (e.g. aspirin and heparin) on ^{18}F-GP1 binding to thrombi was examined in the *in vitro* thrombus model. ^{18}F-GP1 still binds strongly and specifically to thrombi despite the pretreatment with heparin or aspirin. The clot-blood ratio was significantly different between unblocked and blocked ($p<0.01$) under all conditions studied as shown by an unpaired t-test.

The binding characteristics of ^{18}F-GP1 were further analyzed in the blood flow model by continuous signal detection using a PET camera. Immediately after tracer addition, a signal at the thrombus site was measured, increasing throughout the 3min tracer circulation time frame. The signal at the thrombi remained over the entire imaging period (Fig. 4). In one set of experiments excess non-radioactive ^{19}F-GP1 was added to the circuit at 30min and thrombus bound radioactivity was abolished over the next 30min.

Cynomolgus monkey PET imaging

Biodistribution analysis in cynomolgus monkeys showed rapid clearance of ^{18}F-GP1 from healthy tissues and the blood. The tracer concentration measured in the aorta by PET was in good agreement with the activity measured in blood samples. After finishing the imaging study at 60min p.i. the animals were sacrificed and an *ex vivo* organ distribution analysis was performed. Low organ uptake was observed except the gallbladder (Supplemental Figs. 2A and 2B). The maximum intensity projection (MIP) of summed frames from the thorax region obtained directly after injection (0-5min) visualizes the activity in

the main blood vessels. A later time points (40-60min) no detectable signal was observed in the thorax (Supplemental Figs. 2C and 2D).

For the *in vivo* thrombus imaging, a catheter with a roughened thrombogenic area was placed into the left carotid artery of cynomolgus monkeys as shown in a schematic illustration (Fig. 5A). The PET images obtained from all 3 animals examined revealed a strong signal inside the descending aorta along the roughened part of the catheter, with no visible signal associated with the non-roughened catheter and only a sparse signal in the surrounding tissues (Fig. 5B). After removal of the catheters from the animals, a thin layer of thrombi covering the roughened part of the catheter was observed. The thrombogenic volume (1cm length x 0.2cm diameter ~30µL) indicates that the method allows for detection of even small thrombi with high detection sensitivity. No comparison with other standard imaging techniques such as computed tomography pulmonary angiography or ultrasonography was performed in this study. A signal inside the brain was anecdotally noted when scanning other parts of the body after finishing the 60min dynamic scan of the thorax (Fig. 5C). Autopsy revealed a thrombus within the internal carotid artery/Circle of Willis junction (Fig. 5D). It remains unclear if this thrombus detached from the aortic thrombus at the beginning of the experiment (prior tracer injection) or at the end of the experiment (after tracer injection). Therefore it is not yet confirmed that ^{18}F-GP1 can target emboli in the brain, however, the profound spatial resolution was confirmed. In the other studied monkeys, the brains were completely free of any signal. Additional studies are required to assess whether thromboembolic events can be imaged in animal models or humans.

Through insertion of catheters into the right carotid artery and into the vena cava, arterial and venous thrombi were induced in cynomolgus monkeys. Both, the arterial and venous thrombi were equally visualized by ^{18}F-GP1 PET imaging with almost no background from any organ or tissue in the field of view (Fig. 6A). A thin layer of thrombus formation was observed at the roughened areas that showed the same pattern as the PET signals. In the animal shown the left carotid artery was accidentally injured

during the insertion of the catheter into the left jugular vein. This caused an endothelial damage that was confirmed at necropsy. The resulting small thrombotic depositions at the damaged endothelial surface were clearly visualized *in vivo* in the PET image. While unintended, this observation emphasizes that ^{18}F-GP1 is capable of visualizing small arterial thrombi, formed *in situ* within a monkey carotid artery. Time-activity curves confirmed stable binding to both arterial and venous thrombi throughout the 60 min dynamic scan period (Fig. 6B).

DISCUSSION

The development of high affinity, rapidly clearing radiolabeled small-molecules targeting GPIIb/IIIa together with the recent advances in PET-imaging technologies provides an opportunity to overcome the limitations of the previously introduced single photon emission computed tomography agents by detecting thrombi with improved spatial resolution and detection sensitivity. The elarofiban scaffold was selected based on suitable pharmacokinetic properties and feasibility for incorporating the ^{18}F-radiolabel without losing biological activity. Binding studies with either purified GPIIb/IIIa or human thrombus showed that modification of elarofiban with a small fluoro-containing moiety did not affect the binding affinity. In fact, the ^{19}F-GP1 derivative showed in this competition assay a similar IC_{50} value as the parent elarofiban molecule. The measured IC_{50} value of the parent elarofiban in this assay is higher than its reported IC_{50} value using biotinylated fibrinogen in a competition assay (0.4nM) (*13*). As different ligands and conditions were applied these values cannot be directly compared but it can be concluded that the high affinity of elarofiban for GPIIb/IIIa is retained for ^{18}F-GP1.

Species differences in the ligand binding to the GPIIb/IIIa receptors are reported in the literature (*13,16,25,26*) and rodents were shown to be not appropriate for the *in vivo* evaluation of this class of new receptor ligands. Species dependent effects are also reported for elarofiban necessitating the use of

human blood or thrombi for binding studies and autoradiography as well as establishing a non-human primate model for PET imaging of thrombi. Moderate inhibition of platelet aggregation was observed with ^{19}F-GP1. The very low mass dose (<10 µg per dose) applied for radiotracer imaging would result in an initial blood concentration in humans that will be >50-fold below the IC_{50} for aggregation inhibition. Together with the rapid tracer clearance this makes bleeding adverse events extremely unlikely.

An important consideration, which is not addressed well enough in the applied *in vitro* and *in vivo* models, is the target specificity of the current compound compared to previous RGD mimetics. It has been shown that cyclic RGD compounds bind to GPIIb/IIIa as well as other integrins, particularly $\alpha_v\beta_3$. The target $\alpha_v\beta_3$ is present on activated endothelial cells and smooth muscle cells. Other integrins are present on inflammatory cells. This may explain why agents like apcitide show a diffuse soft tissue uptake in the vicinity of the DVT. Elarofiban has shown a >300,000-fold specificity for GPIIb/IIIa over $\alpha_v\beta_3$ (*27*) and it can be postulated that the thrombus is better visualized using an elarofiban derivative without obfuscation by the surrounding inflamed tissue in man. Higher target specificity should also allow a more accurate detection of pathological mechanisms in atherosclerosis where both platelets and vascular cells are implicated. In principle it will also improve the discrimination between infectious and thrombogenic events (e.g. endocarditis, valvular vegetations), although this has yet to be tested.

The human *ex vivo* blood circuit is a simple model to study clot formation *in vitro* and is very flexible, allowing investigations of different blood-species, anticoagulants, and flow rates. Coupling the blood circuit to a PET camera allows real time quantification of clot binding and retention. Especially measurements under arterial flow rates were used to maximize the adhesion of activated platelets. The combined results of abrogation of tracer binding to the clot by addition of excess unlabeled GP1 or elarofiban and un-affected clot accumulation of ^{18}F-GP1 under aspirin or heparin treatment confirm specific tracer binding. Real time assessment when the nidus was placed inside a PET camera recapitulated

the results, and furthermore, confirmed the rapid accumulation and visualization of the retained ^{18}F-GP1 on the clot.

Preclinical proof of *in vivo* thrombus imaging was obtained after insertion of analogously prepared roughened polyethylene catheters into the primate arterial system and into the venous system. Even small thrombi were easily and distinctly visualized at the roughened catheter region. The ability to image small thrombi was confirmed by the observation in one animal in which the carotid artery was inadvertently damaged during catheter placement. This recapitulated a "real-life" situation and showed that ^{18}F-GP1 was able to visualize naturally occurring thrombi. The intra-cerebral clot visualization was opportunistic, but gave insight into the possible capabilities of ^{18}F-GP1. It cannot be confirmed whether ^{18}F-GP1 was injected before or after the arterial thrombus was displaced and lodged in the brain. Nonetheless, it represents the visualization of a very small clot lodged in the middle cerebral artery and bodes well for the possibility of imaging strokes /cerebrovascular accidents in humans.

CONCLUSIONS

^{18}F-GP1 is a promising novel PET tracer for thrombus imaging *in vitro* and *in vivo*. It binds with high affinity to GPIIb/IIIa, the key receptor for platelet aggregation. Strong binding was observed on an explanted human cardiac thrombus, in the *in vitro* human blood-flow-thrombus model and on platelet depositions on catheter and endothelium surfaces as well as on emboli in cynomolgus monkeys confirming its potential for PET imaging of such thrombogenic events. Efficacy was not altered by anticoagulation therapy. A favorable biodistribution profile supports the translation of ^{18}F-GP1 into the clinic. A first-in-man study is currently ongoing and further conclusions await clinical trial results.

ACKNOWLEDGMENTS

The authors thank Robert Ivkic, Martin Kohs, Violetta Sudmann, Lorenz Behringer, Samira Leesch for their motivation, excellent work and skilled technical assistance. Furthermore, the authors thank Anna-Lena Frisk for performing histopathology examinations and the Heart and Diabetes Center Bad Oeynhausen for providing an explanted human thrombus. The platelet aggregation data was kindly provided by Christoph Gerdes (TRG Cardiology, Bayer Pharma, Wuppertal).

Sources of Funding

This work was funded by Bayer Pharma AG and Piramal Imaging GmbH, Berlin, Germany.

Disclosures

Andrew Stephens, Mathias Berndt, Andre Müller, Norman Koglin, Felix Oden, Marion Zerna, Matthias Friebe and Ludger Dinkelborg are employees of Piramal Imaging GmbH, Berlin, Germany. Jessica Lohrke, Holger Siebeneicher, Markus Berger, Marcus Bauser, Joachim Hütter are employees of Bayer Pharma AG, Berlin, Germany.

REFERENCES

1. Mozaffarian D, Benjamin EJ, Go AS, et al. Heart disease and stroke statistics-2016 update: A report from the American Heart Association. *Circulation.* 2016;133:e38-360.

2. Pomero F, Dentali F, Borretta V, et al. Accuracy of emergency physician-performed ultrasonography in the diagnosis of deep-vein thrombosis: a systematic review and meta-analysis. *Thromb Haemost.* 2013;109:137-145.

3. Lee W. General principles of carotid Doppler ultrasonography. *Ultrasonography.* 2014;33:11-17.

4. Srichai MB, Junor C, Rodriguez LL, et al. Clinical, imaging, and pathological characteristics of left ventricular thrombus: a comparison of contrast-enhanced magnetic resonance imaging, transthoracic echocardiography, and transesophageal echocardiography with surgical or pathological validation. *Am Heart J.* 2006;152:75-84.

5. Fedullo PF, Tapson VF. Clinical practice. The evaluation of suspected pulmonary embolism. *N Engl J Med.* 2003;349:1247-1256.

6. Righini M, Le Gal G, Aujesky D, et al. Diagnosis of pulmonary embolism by multidetector CT alone or combined with venous ultrasonography of the leg: a randomised non-inferiority trial. *Lancet.* 2008;371:1343-1352.

7. Ciesienski KL, Caravan P. Molecular MRI of thrombosis. *Curr Cardiovasc Imaging Rep.* 2010;4:77-84.

8. Zierler BK. Ultrasonography and diagnosis of venous thromboembolism. *Circulation.* 2004;109:I9-14.

9. Stein PD, Fowler SE, Goodman LR, et al. Multidetector computed tomography for acute pulmonary embolism. *N Engl J Med.* 2006;354:2317-2327.

10. Sweet PH, 3rd, Armstrong T, Chen J, Masliah E, Witucki P. Fatal pulmonary embolism update: 10 years of autopsy experience at an academic medical center. *JRSM Short Rep.* 2013;4:2042533313489824.

11. Nurden P, Poujol C, Durrieu-Jais C, et al. Labeling of the internal pool of GP IIb-IIIa in platelets by c7E3 Fab fragments (abciximab): flow and endocytic mechanisms contribute to the transport. *Blood.* 1999;93:1622-1633.

12. Cook JJ, Bednar B, Lynch JJ, et al. Tirofiban (Aggrastat®). *Cardiovascular Drug Reviews.* 1999;17:199-224.

13. Damiano BP, Mitchell JA, Giardino E, et al. Antiplatelet and antithrombotic activity of RWJ-53308, a novel orally active glycoprotein IIb/IIIa antagonist. *Thromb Res.* 2001;104:113-126.

14. Hoekstra WJ, Beavers MP, Andrade-Gordon P, et al. Design and evaluation of nonpeptide fibrinogen gamma-chain based GPIIb/IIIa antagonists. *J Med Chem.* 1995;38:1582-1592.

15. Hoekstra WJ, Maryanoff BE, Damiano BP, et al. Potent, orally active GPIIb/IIIa antagonists containing a nipecotic acid subunit. Structure-activity studies leading to the discovery of RWJ-53308. *J Med Chem.* 1999;42:5254-5265.

16. Maryanoff BE. Adventures in drug discovery: potent agents based on ligands for cell-surface receptors. *Acc Chem Res.* 2006;39:831-840.

17. Scarborough RM, Gretler DD. Platelet glycoprotein IIb-IIIa antagonists as prototypical integrin blockers: novel parenteral and potential oral antithrombotic agents. *J Med Chem.* 2000;43:3453-3473.

18. Houshmand S, Salavati A, Hess S, Ravina M, Alavi A. The role of molecular imaging in diagnosis of deep vein thrombosis. *Am J Nucl Med Mol Imaging.* 2014;4:406-425.

19. Lister-James J, Knight LC, Maurer AH, Bush LR, Moyer BR, Dean RT. Thrombus imaging with a technetium-99m-labeled activated platelet receptor-binding peptide. *J Nucl Med.* 1996;37:775-781.

20. Douketis JD, Ginsberg JS, Haley S, et al. Accuracy and safety of (99m)Tc-labeled anti-D-dimer (DI-80B3) Fab' fragments (ThromboView(R)) in the diagnosis of deep vein thrombosis: a phase II study. *Thromb Res.* 2012;130:381-389.

21. Morris TA, Gerometta M, Yusen RD, et al. Detection of pulmonary emboli with 99mTc-labeled anti-D-dimer (DI-80B3)Fab' fragments (ThromboView). *Am J Respir Crit Care Med.* 2011;184:708-714.

22. Blasi F, Oliveira BL, Rietz TA, et al. Radiation dosimetry of the fibrin-binding probe (64)Cu-FBP8 and its feasibility for PET imaging of deep vein thrombosis and pulmonary embolism in rats. *J Nucl Med.* 2015;56:1088-1093.

23. Breddin HK. Can platelet aggregometry be standardized? *Platelets.* 2005;16:151-158.

24. Sukavaneshvar S. Assessment and management of vascular implant thrombogenecity. In: Wakhloo AK GM, Lieber BB, ed. *Thrombus and stroke*. New York: Informa Healthcare; 2008:57-77.

25. Basani RB, Zhu H, Thornton MA, et al. Species differences in small molecule binding to alpha IIb beta 3 are the result of sequence differences in 2 loops of the alpha IIb beta propeller. *Blood.* 2009;113:902-910.

26. Harfenist EJ, Packham MA, Mustard JF. Effects of the cell adhesion peptide, Arg-Gly-Asp-Ser, on responses of washed platelets from humans, rabbits, and rats. *Blood.* 1988;71:132-136.

27. De Corte BL, Kinney WA, Liu L, et al. Piperidine-containing beta-arylpropionic acids as potent antagonists of alphavbeta3/alphavbeta5 integrins. *Bioorg Med Chem Lett.* 2004;14:5227-5232.

Figures

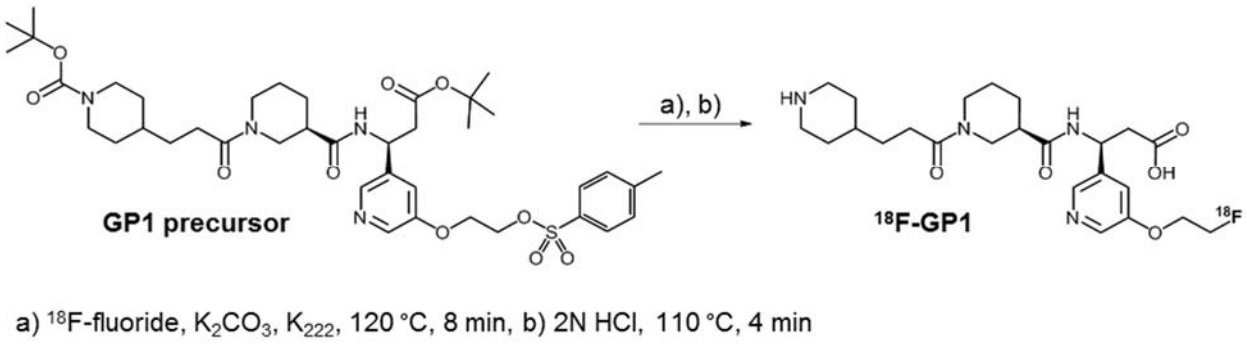

FIGURE 1. Radiosynthesis of ^{18}F-GP1 was performed starting from the Boc-protected tosylate precursor (GP1 precursor). A two-step synthesis followed by purification afforded 1.8–3.5 GBq ^{18}F-GP1 (yield 39±4% decay corrected, radiochemical purity > 99%) in 81–84 min overall preparation time (n=3).

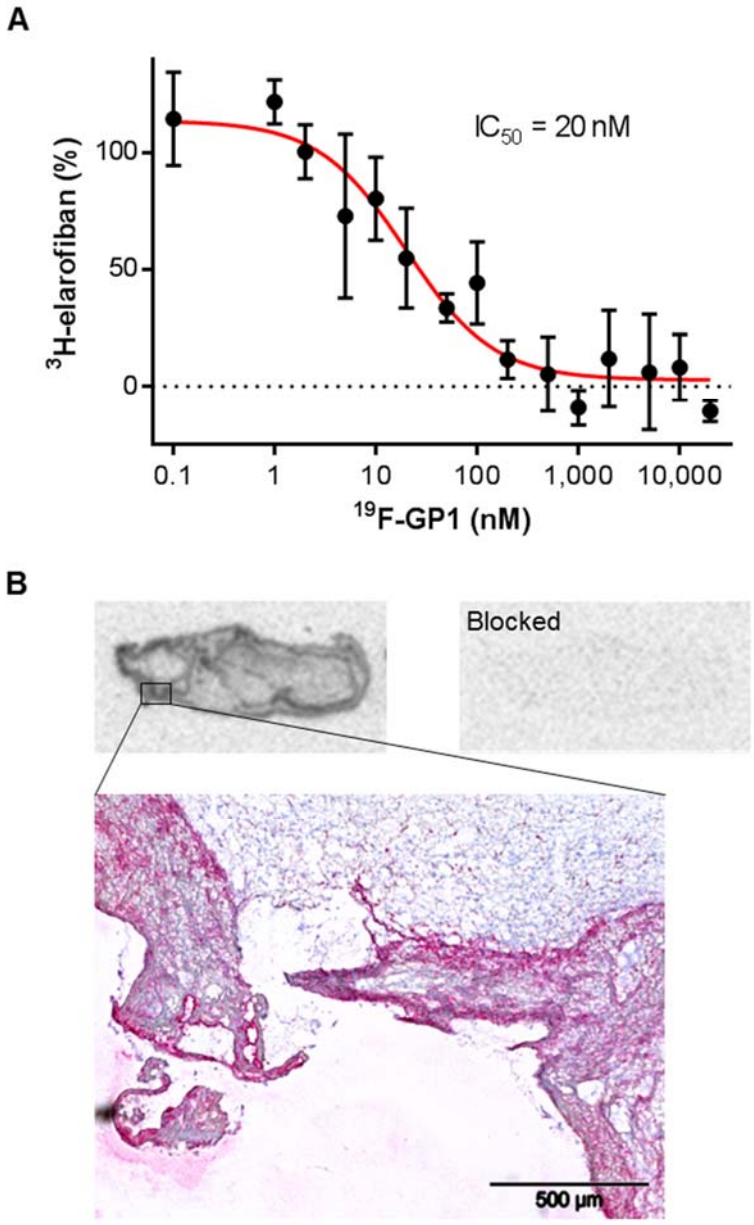

FIGURE 2. Binding characteristics of ^{19}F-GP1 and ^{18}F-GP1. (A) IC_{50} measurement of the non-radioactive ^{19}F-GP1 derivative on microtiter plates coated with human GPIIa/IIIb. (B) Autoradiography using ^{18}F-GP1 on a slice of a clinical left ventricular thrombus explanted from a human heart. The CD41 (GPIIb) staining is shown below.

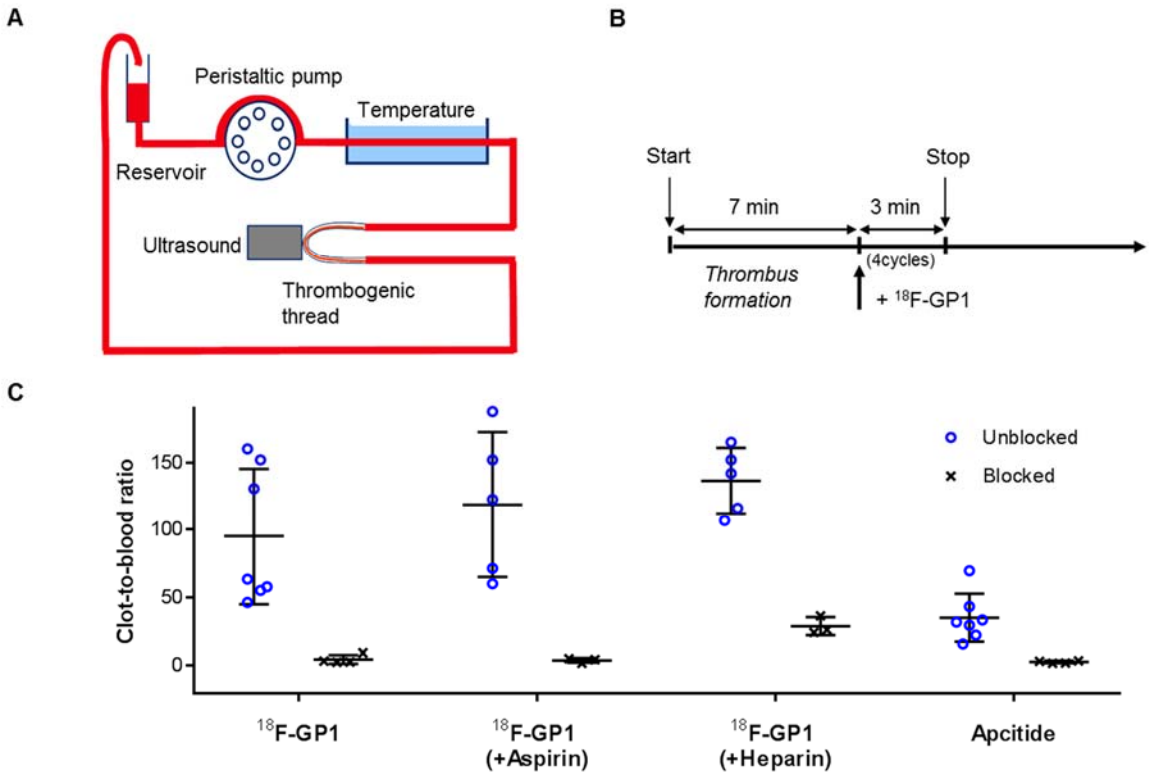

FIGURE 3. Determination of clot-blood ratios using an *in vitro* blood flow model. The experimental setup is shown in (A) and the sequence and duration of steps is shown in (B). Clot-to-blot ratios were determined for ^{18}F-GP1 and apcitide under different conditions (C). The clot-blood ratio was significantly different between unblocked and blocked under all conditions studied as shown by an unpaired t-test ($p<0.01$).

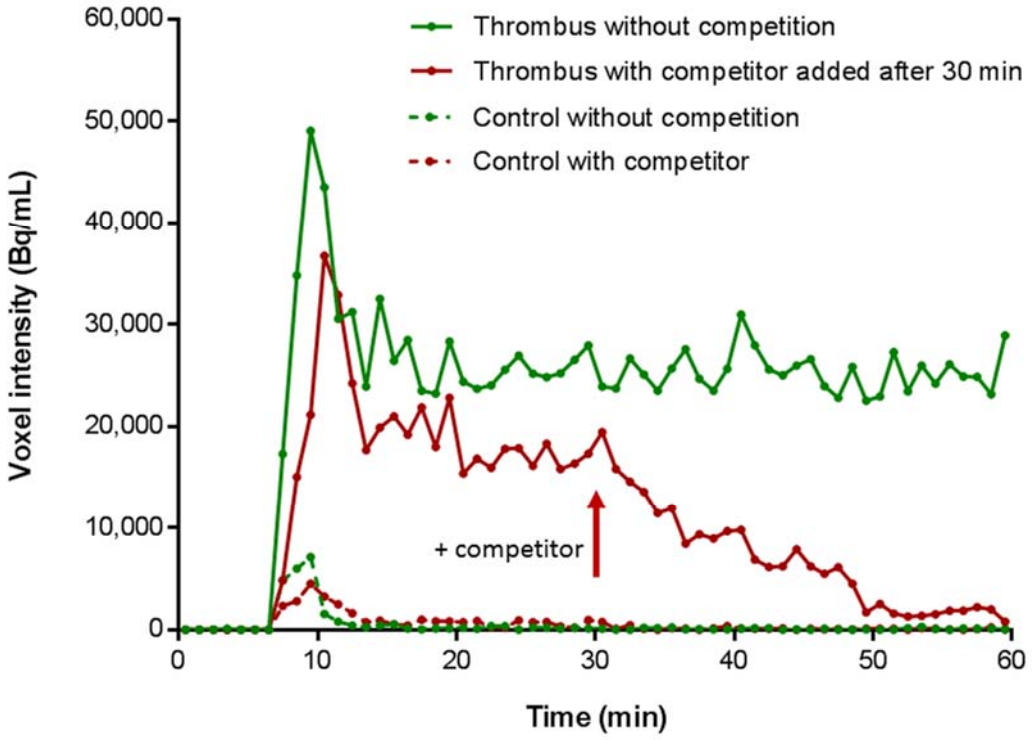

FIGURE 4. PET imaging of ^{18}F-GP1 thrombus binding in the *in vitro* blood flow model (representative time activity curves shown). A strong signal was measured in the thrombus region directly after tracer addition at 7min whereas low signal was measured in the control area (dashed lines). ^{18}F-GP1 remained bound to the thrombus over the whole imaging procedure . After addition of excess non-radioactive ^{19}F-GP1 at 30min a complete displacement of thrombus bound signal was observed until 60min .

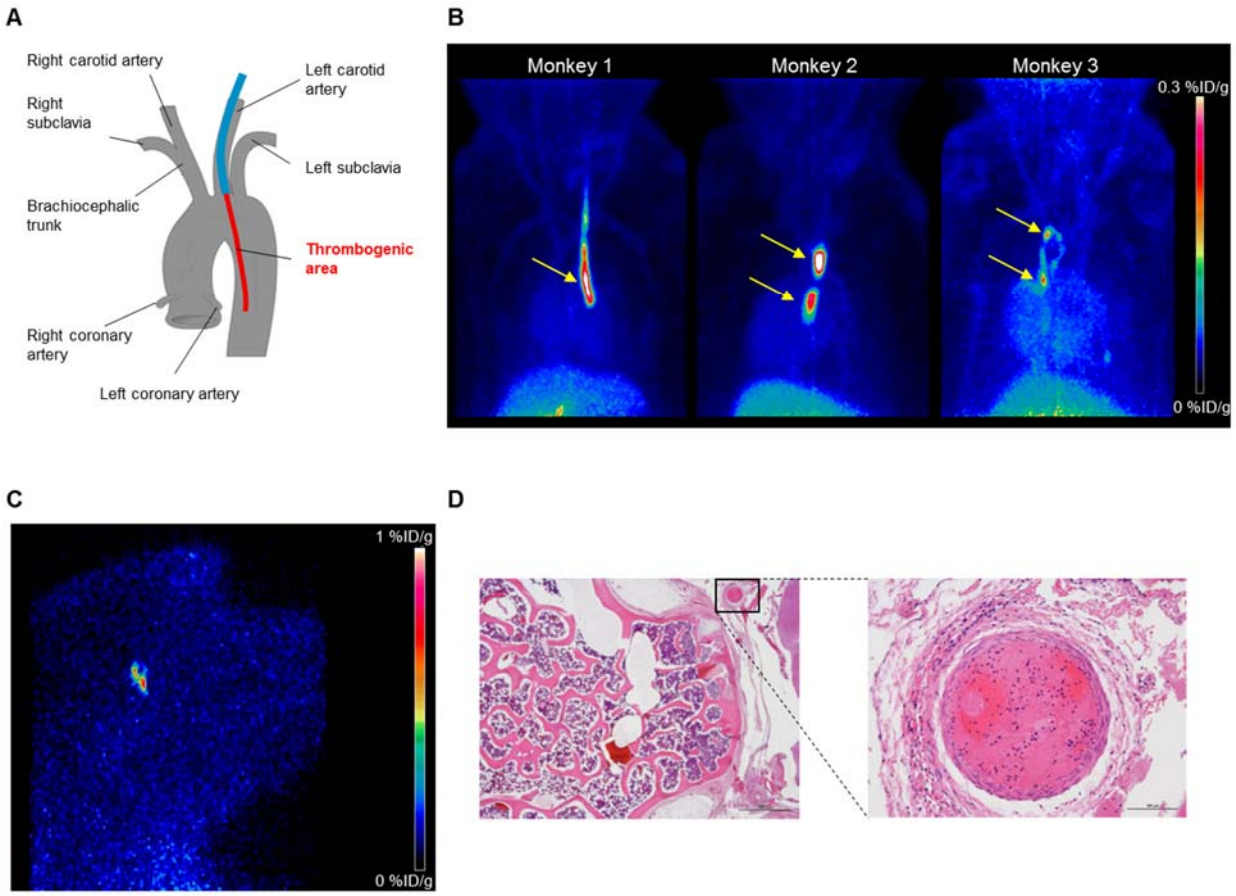

FIGURE 5. PET imaging of arterial thrombi with ^{18}F-GP1 in cynomolgus monkeys. (A) Schematic illustration of the location of the advanced catheter in the descending aorta. (B) PET images (MIP 0-60min) of three cynomolgus monkeys. Strong signals are detected at the sites where catheters with roughened surfaces were introduced. Almost no other background signal is visible. Only accumulation in the gallbladder becomes visible at the bottom of the image. (C) Suspect PET imaging finding inside the brain of monkey 2 measured after the 60min dynamic scan of the thorax. (D) The finding observed in C was confirmed as thrombus inside the internal carotid artery / Circle of Willis junction by pathology.

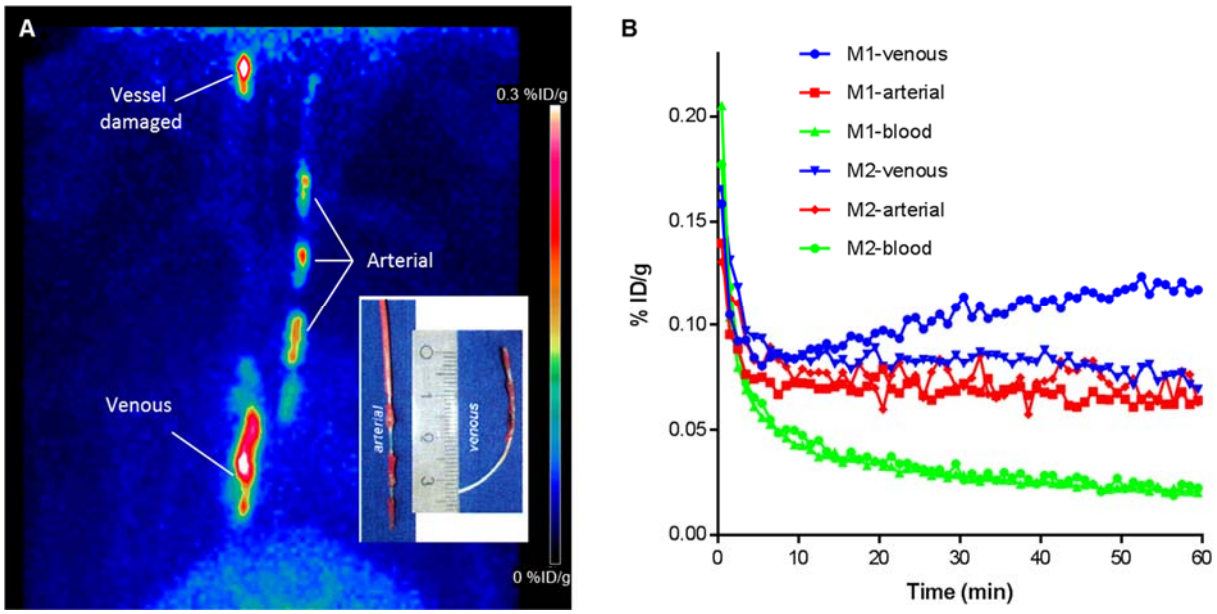

FIGURE 6. (A) ^{18}F-GP1 PET-image (MIP 0-60min) of a cynomolgus monkey with an arterial and a venous catheter that were introduced in the right carotid artery and into the vena cava, respectively. Tracer uptake was visualized in both the arterial and venous thrombi in both animals investigated with two catheters. (B) Time-activity curves of ^{18}F-GP1 thrombus uptake and blood clearance from the monkey 1 shown in (A) and monkey 2.

Supplemental information

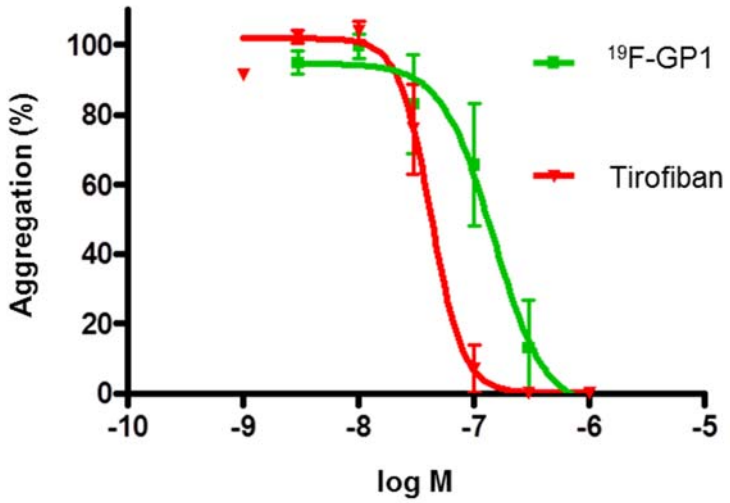

SUPPLEMENTAL FIGURE 1. Investigation of human platelet rich plasma aggregation after adenosine diphosphate stimulus during incubation with ^{19}F-GP1 and tirofiban.

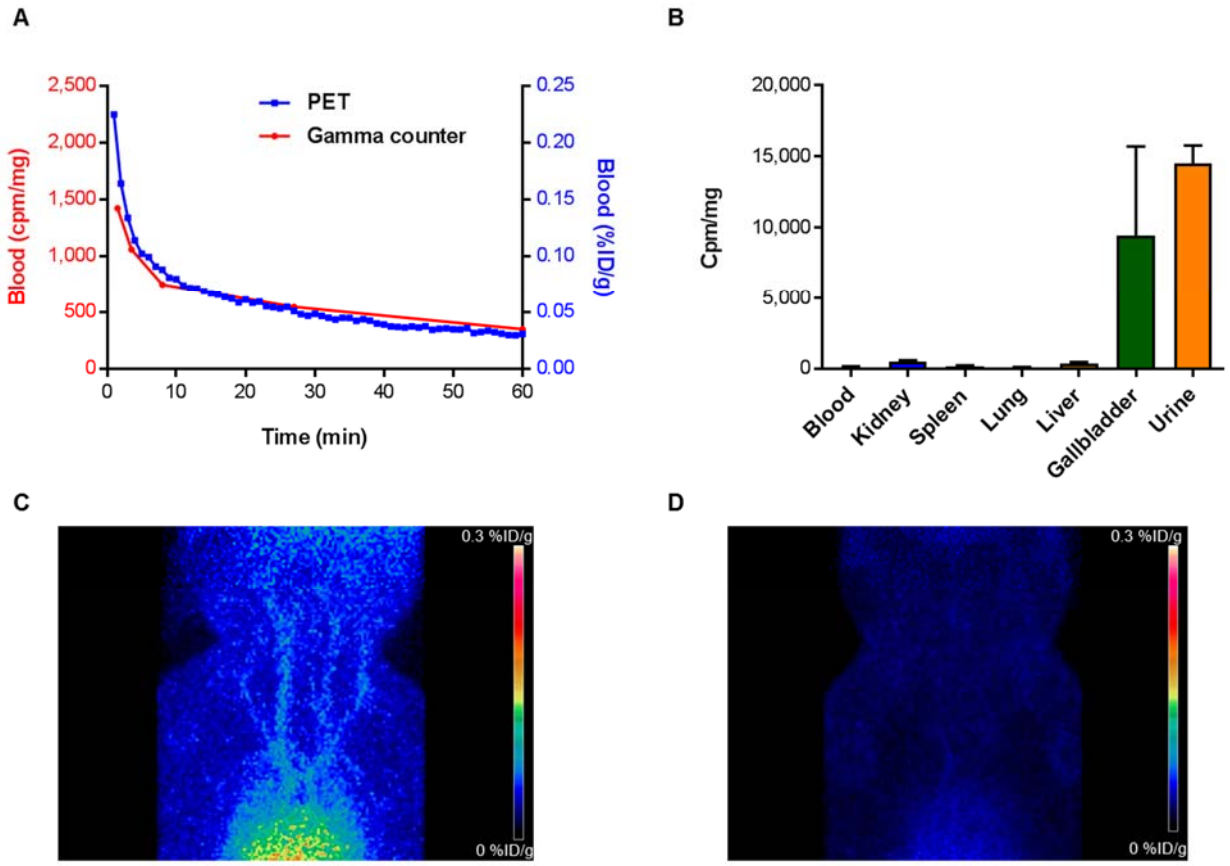

SUPPLEMENTAL FIGURE 2. Biodistribution and pharmacokinetic analyses of ^{18}F-GP1 in cynomolgus monkeys. (A) Activity measured in blood samples and by PET are in good agreement. (B) *Ex vivo* organ distribution in cynomolgus monkeys. Only low amounts of radioactivity was measured in blood, kidney, spleen, lung and liver at this time point. The high amounts of radioactivity measured in urine and gallbladder indicate a rapid renal and partial hepatobiliary clearance. (C) MIP images of the thorax and heart region from 0-5min and (D) 40-60min post injection showing rapid clearance and low tissue background of ^{18}F-GP1.